An Electronically Controlled Leaky-Wave Antenna Based on Corrugated SIW Structure With Fixed-Frequency Beam Scanning

Ke Chen, Yun Hua Zhang, Si Yuan He, Hai Tao Chen, and Guo Qiang Zhu

***Abstract*—A novel electronically controlled (EC) leaky-wave antenna (LWA) based on corrugated substrate integrated waveguide (CSIW) with fixed-frequency beam-steerable capability is presented in this letter. This structure is based on a CSIW structure with rectangular ring slots and metallic vias to the ground, which realizes two isolated dc equipotential planes. Each slot of the rectangular ring is loaded with a varactor diode, and thus the series and shunt capacitance are tunable by adjusting the dc bias voltage, which eventually results in beam scanning at a fixed frequency. The proposed antenna is a single-layer structure and has a simplified dc bias network, which merely needs an inductor and a short microstrip line. An EC beam-steerable CSIW LWA is designed and experimentally validated. It is experimentally demonstrated that the radiation angle ranges from −40.66° to 31.32° as the bias voltage is tuned from 32 V to 7.5 V at 4.5 GHz.**

***Index Terms*—Corrugated substrate integrated waveguide (CSIW), fixed-frequency beam-steerable, leaky-wave antenna (LWA).**

I. Introduction

PLANAR leaky-wave antennas (LWAs) have attracted much attention in wireless communication systems due to their low-profile, frequency-scanning capability, and ease of feeding [1]. However, the main beam of conventional LWAs can only scan in the forward quadrant or backward quadrant. Quasi-uniform and -1-order mode LWAs are proposed to obtain continuous beam scanning from backward to forward [2], [3].

Recently, LWAs based on substrate integrated waveguide (SIW) have raised significant research attention due to low loss, high-power capacity, and ease of fabrication [3], [4]. Furthermore, SIW, half-mode SIW (HMSIW), HMSIW with spoof surface plasmon polariton (SSPP), and corrugated SIW (CSIW) structures are applied to realize LWAs with frequency scanning capability [4]–[8]. Compared to the HMSIW and HMSIW-SSPP structure, the CSIW structure without metallic vias to the ground, which makes have the potential to design a simplified dc bias network.

However, frequency-dependent LWAs have suffered a limitation because most modern wireless communication systems operate in a fixed frequency band. Fixed-frequency beam-steerable can be achieved by using p-i-n diodes as switches to control phase shift, but it is limited to several discrete radiation angles [9]. Continuous beam scanning controlled LWAs have been achieved by coplanar waveguide based continuous transverse stubstructure or Fabry–Pérot structure [10], [11], but those antennas need a high profile. Backward to forward scanning electronically controlled (EC) LWA has been obtained in composite right/left-handed transmission line (CRLH-TL) loaded with varactor diodes [12]. A circularly polarized LWA based on CRLH-TL structure with the square-shaped patch is presented in [13]. However, the radiation efficiency is not high due to the loss of microstrip (MS) structure, and the dc bias network is quite complex. To obtained fixed-frequency beam-steerable with high radiation efficiency, some HMSIW-based LWAs have been designed [14], [15]. However, the LWA in [14] is not able to realize electronically control due to no dc bias network. Furthermore, the LWA in [15] relies on multilayer substrates and complex dc bias network, which is hard to fabricate. In order to overcome those drawbacks, a novel LWA based on CSIW structure with the advantage of ease to fabricate is proposed [8].

In this letter, a beam tunable LWA based on CSIW at a fixed frequency is proposed. By introducing rectangular ring slots and metallic vias on CSIW structure, two isolated dc equipotential planes on a single-layer are obtained. Each rectangular ring slot is loaded with four varactor diodes, and thus the series and shunt capacitance are tunable by changing the dc bias voltage, which eventually results in beam scanning at a fixed frequency. The proposed LWA is easy to fabricate owing to its single-layer structure and extremely simplified dc bias network.

The proposed antenna structure and analysis are described in detail in Section II. Full-wave analysis and the measured results are shown in Section III. Finally, a conclusion is drawn in Section IV.

II. Antenna Design and Analysis

The CSIW structure is using quarter-wave open-circuit MS stubs in place of metallic vias to offer electric sidewalls. So the CSIW structure confines energy transmission in the same

Manuscript received December 10, 2018; revised January 7, 2019; accepted January 26, 2019. Date of publication January 30, 2019; date of current version March 1, 2019. This work was supported by the National Nature Science Foundation of China under Grant 61301061. *(Corresponding author: Yun Hua Zhang.)*

K. Chen, Y. H. Zhang, S. Y. He, and G. Q. Zhu are with the School of Electronic Information, Wuhan University, Wuhan 430072, China (e-mail: 2013202120030@whu.edu.cn; zhangyunhua@whu.edu.cn; siyuanhe@whu.edu.cn; gqzhu@whu.edu.cn).

H. T. Chen is with the Wuhan Maritime Communication Research Institute, Wuhan 430079, China (e-mail: hbcht@163.com).

Digital Object Identifier 10.1109/LAWP.2019.2896354

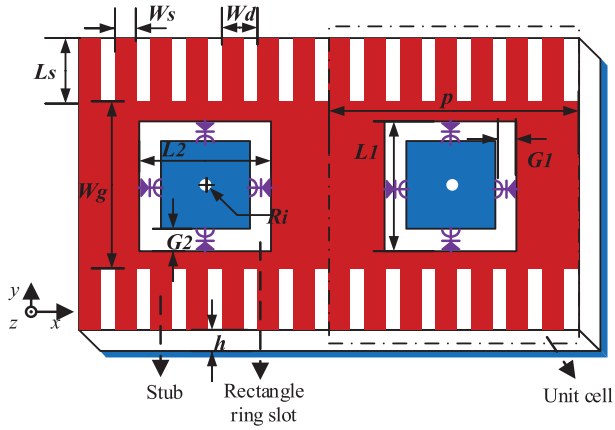

Fig. 1. Scheme of the proposed CSIW-based unit cell. $L_s = 15$ mm, $W_g = 30$ mm, $W_s = 1$ mm, $W_d = 2$ mm, $L_1 = 18$ mm, $L_2 = 10.5$ mm, $G_1 = 0.8$ mm, $G_2 = 0.8$ mm, $R_i = 0.3$ mm, $p = 20$ mm, $h = 1$ mm, and $\varepsilon_r = 3.55$.

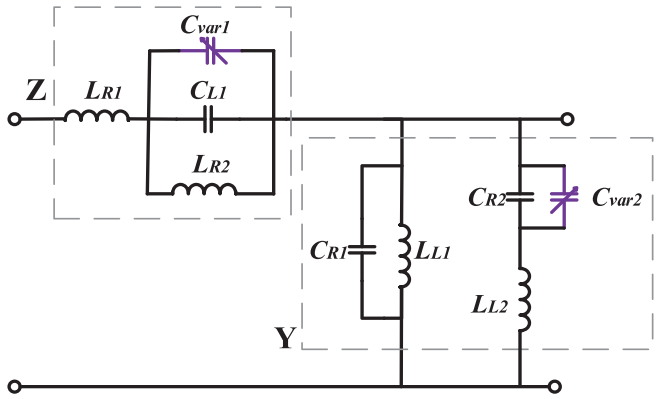

Fig. 2. Equivalent circuit of unit cell.

manner as that of the SIW. The method to calculate the equivalent width of the CSIW structure can be simplified as a dielectric-filled waveguide similar to SIW [16]. Besides, the length of MS open-circuit stubs is a quarter wavelength at the center frequency. It should be noted that the propagation mode is quasi-TEM mode when the MS open-circuit stub is much less than the quarter wavelength [17].

Fig. 1 shows the scheme of the proposed LWA based on CSIW structure. The unit cell includes four varactors and a CSIW structure with a rectangular ring slot. By implemented rectangular ring slots and metallic vias on the top plane, two isolated dc equipotential planes on a single-layer are obtained. Four varactor diodes are loaded on each rectangular ring slot, and the series and shunt capacitor of varactors are tunable by adjusting the dc bias voltage. Moreover, the red color is one dc equipotential plane used for dc bias, and the blue color for the ground plane. So the dc bias network will be extremely simplified.

In order to realize the beam scanning of LWA from backward to forward at principal mode, the proposed CSIW structure must possess propagation characteristic similar to CRLH-TL structure. So the proposed antenna should operate near or below the cutoff frequency of the main waveguide to obtain the left-handed propagation behavior [2]. And the radiation angle of quasi uniform LWA can be calculated as

$$\theta = sin^{-1}\left(\beta/k_0\right) \tag{1}$$

where β is the phase constant and k_0 is the propagation constant of free space. When $\beta < k_0$, the proposed structure is in fast wave region and the mode from guide wave mode to leak wave.

The equivalent circuit model of unit cell structure is obtained as shown in Fig. 2, which consists of series impedance Z and shunt admittance Y. Here, varactor diodes are simplified as a capacitor adjusted by reverse voltage. And the propagation constant can be calculated as follows [2]:

$$\beta p = cos^{-1}\left(1 + Z\left(V\right)Y\left(V\right)\right) \tag{2}$$

where the series impedance Z includes series capacitor and series inductor. The rectangular ring slots and the two series varactors offer the series capacitor C_{L1} and C_{var1}, while the patch of top plane provides the equivalent series inductor L_{R1} and L_{R2}. Similarly, shunt capacitor and shunt inductor make up the shunt admittance Y. The patch of top plane, the rectangular ring slots, and the two shunt varactors offer shunt capacitor C_{R1}, C_{R2}, and C_{var2}. And the metallic vias and open-circuit stubs provide the shunt inductor L_{L1} and L_{L2}. By changing the reverse voltage, the series and shunt capacitance of varactors can be adjusted, and then the β becomes tunable by the reverse voltage.

The primary zero points of Z and Y can be written as follows:

$$\omega_{se} = \frac{1}{C_{L1} + C_{\mathrm{var1}}}\left(\frac{1}{L_{R1}} + \frac{1}{L_{R2}}\right) \tag{3}$$

$$\omega_{\mathrm{sh}} = \frac{1}{L_{L1}\left(C_{R1} + C_{R2} + C_{\mathrm{var2}}\right)} \tag{4}$$

where those equivalent circuit parameters can be extracted from simulated S-parameters. $C_{\mathrm{var1}} = C_{\mathrm{var0}}/2$ and $C_{\mathrm{var2}} = 2C_{\mathrm{var0}}$, meanwhile C_{var0} is the capacitance of the varactor diode. When the C_{var0} increases, the ω_{se} and the ω_{sh} will decrease simultaneously. At a fixed frequency ω_0, the balanced frequency $\omega_b = \sqrt{\omega_{se}\omega_{\mathrm{sh}}}$ can be lower than, equal to or higher than the ω_0 by changing the values of C_{var0}. Thus the value of β from negative, to zero, then to positive at a fixed frequency is achieved. It is noteworthy that short-open calibration can be employed to eliminate the high-order mode effects and port discontinuities, thus obtaining accurately complex propagation constants [17].

In Fig. 3, the propagation constants are plotted at $C_{\mathrm{var0}} = 0.4$ pF, 0.45 pF, and 0.5 pF. From Fig. 3(a), backward and wave propagation can be obtained over 4.4–4.55 GHz and 4.4–4.7 GHz when the C_{var0} values are 0.4 and 0.5 pF, respectively. And $\beta = 0$ at 4.5 GHz is achieved when the C_{var0} is 0.45 pF. So the radiation angle from forward, broadside or backward at 4.5 GHz is achieved by changing the value of C_{var0}. At 4.5 GHz, the attenuation constant of backward-wave is larger than forward-wave, as shown in Fig. 3(b). The propagation constant has some fluctuations at low frequency region for this structure is near the cutoff frequency of the CSIW and still exist a narrow open-stopband.

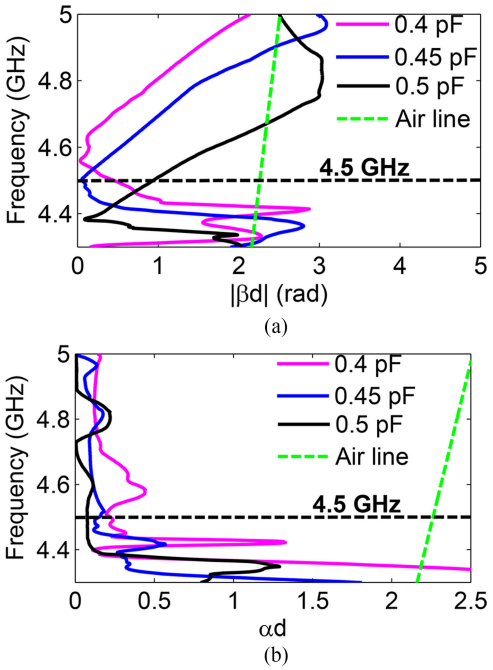

Fig. 3. Complex propagation constant of the proposed LWA unit cell at C_{var0} = 0.4 pF, 0.45 pF, and 0.5 pF. (a) Phase constant. (b) Attenuation constant.

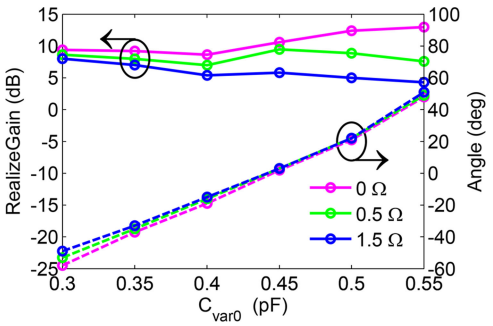

Fig. 4. Simulated gain (solid lines) and angle (dashed lines) for different values of internal resistance R_{s} of the varactor diode.

III. Simulated and Measured Results

A. Simulation Analysis

In order to satisfy the capacitance range in Section II, SMV1430-079LF varactor diodes are used in the design of CSIW-based EC LWA, and C_{var0} varies in the range of 0.3–0.55 pF. It is noted that the internal resistance R_s of each varactor is a bit large and about 1.5 Ω.

Then, the ten cells cascaded EC LWA based on CSIW structure with different values of internal resistance R_s is simulated, as shown in Fig. 4. When $R_{\mathrm{s}} = 0$, the simulated realized gains are better than 8.6 dB, and the maximum gain is 12.8 dB. Meanwhile, the beam scanning is at least from −58° to 48° as the C_{var0} from 0.3 pF to 0.55 pF. In addition, the total efficiencies of antenna are 0.78, 0.92, and 0.76 when the C_{var0} are 0.5, 0.44, and 0.32 pF, respectively. With the R_s increasing from 0 Ω to 1.5 Ω, the realized gains of the backward radiation region have a bit decrease and the realized gains of the forward radiation region decrease rapidly. The reason for this is that the attenuation constant of the backward radiation region is larger than those of the forward radiation. And the beam angles are staying almost the same when the R_s changes from 0 Ω to 1.5 Ω. It is demonstrated that the realized gain of the proposed antenna can be significantly influenced by the ohmic losses of varactors.

Fig. 5. Photograph of the fabricated EC CSIW LWA.

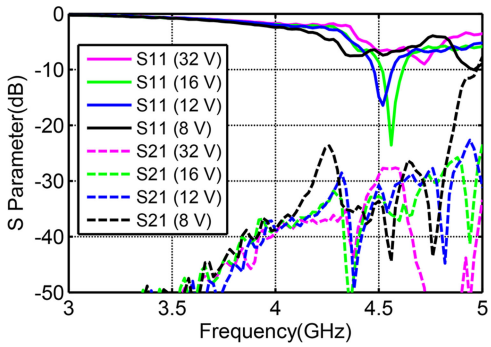

Fig. 6. Measured *S*-parameters at different reverse bias voltages V = 32 V, 16 V, 12 V, and 8 V.

B. Experimental Results

For verification, an EC CSIW LWA cascaded by ten unit cells is fabricated, as shown in Fig. 5. The fabricated antenna is a single-layer substrate and has a simplified dc bias network, which merely needs an inductor, a short MS line. The antenna prototype is manufactured by Rogers 4003c substrate ($\varepsilon_{\mathrm{r}} = 3.55$), and the whole size is 240 mm × 60 mm × 1 mm. Skyworks SMV1430-079LF varactor diodes are utilized to implement unit cells structure, and Murata chip inductor with 20 nH is used for dc bias. The internal resistance R_{s} of each varactor is about 1.5 Ω. A tapered MS line is employed to feed the proposed antenna for impedance match [18].

The measured *S*-parameters are shown in Fig. 6. According to Fig. 6, S_{21} is almost below −25 dB at 4.5 GHz due to the ohmic losses of varactors. Meanwhile S_{11} is −14.9, −9.1, −7.0, and −6.7 dB at the bias voltage is 8 V, 12 V, 16 V, and 32 V, respectively. The difficulty of matching to the conventional 50 Ω transmission line for the backward scanning cases is due to the large bloch impedance. By optimizing the tapered MS line, the better impedance match could be obtained.

The comparison between the measured and simulated results of realized gain and beam angle as shown in Fig. 7. It is shown that, at 4.5 GHz, the measured results of radiation angles are in good agreement with the simulated results at all bias volt-

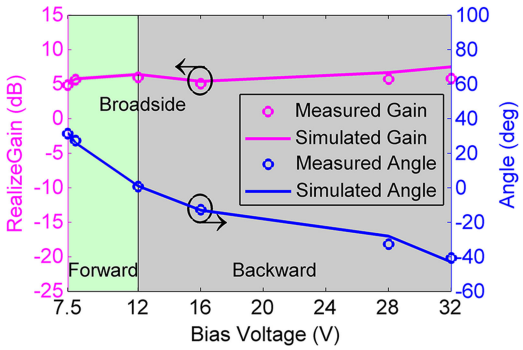

Fig. 7. Realized gain and beam angle of the proposed antenna at 4.5 GHz as bias voltage changes (both simulated and measured).

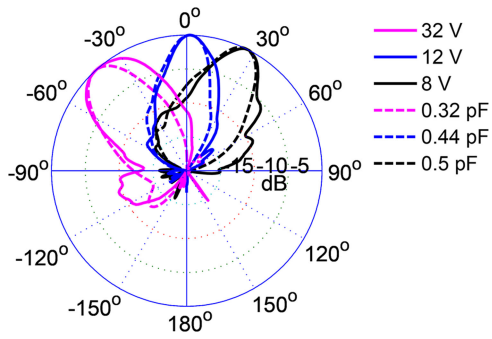

Fig. 8. Measured and simulated radiation patterns in the *E* plane at 4.5 GHz. The measurement results are solid line and the simulation results are dashed line.

ages. And the radiation angle is 31.32°, 27.3°, 0.68°, −12.7°, −32.65°, and −40.66° at the different reverse voltages 7.5, 8, 12, 16, 28, and 32 V, respectively. The radiation angle is scanning from forward to backward as the bias voltage increases. The measured results of antenna gain are about 1 dB lower than the simulated results in some regions, which is due to the dimensional tolerance and material loss. And the measured results of realized gain are 4.9, 5.6, 6, 5.1, 5.7, and 5.8 dB at the different reverse voltages 7.5, 8, 12, 16, 28, and 32 V, respectively. The measured results demonstrate that the beam scans from −40.66° to 31.32° as the bias voltage increases from 7.5 V to 32 V with broadside radiation at 12 V, and the measured results of gain are almost better than 5 dB.

The measured and simulated normalized radiation patterns of *E* plane at 4.5 GHz are depicted in Fig. 8, showing a good agreement. The measured beamwidth of backward radiation is slightly broaden than the simulated beamwidth, which is due to the loss the dimensional tolerance and the capacitance shift of varactors. And the measured efficiencies of the antenna are 0.17, 0.26, and 0.28 at the different reverse voltages 7.5, 12, and 32 V, respectively. Due to the ohmic losses of varactors and material loss, the measured efficiencies are much lower than simulated efficiencies.

Finally, in Table I, the performance of the proposed antenna is compared to other recently continuous fixed-frequency beam-steerable LWAs [10], [12], and [13], where EFF is the efficiency of the antenna. Compared to [10], the proposed antenna is an EC antenna and have a low profile. It is noted that the fixed-capacitor

TABLE I
PERFORMANCE COMPARISON OF DIFFERENT CONTINUOUS FIXED-FREQUENCY BEAM-STEERABLE LWAS

	[10]	[12]	[13]	This work
Operate frequency	2.4 GHz	3.3 GHz	2.4 GHz	4.5 GHz
Range	58~124°	-49~50°	-17~40°	-41~31°
Range (Gain>5dB)	58~124°	-49~14°	-7~15°	**-41~31°**
Average Gain	9.7 dBi	6 dBi	4.9 dBi	5.6 dBi
Max EFF	0.39	N/A	0.22	0.28
Number of diodes	Fixed capacitor	90	60	**40**
Size (λ_0)	0.5	2.2	3.25	3.6
Height	30 mm	1.6 mm	1 mm	1 mm
Technology	CPW-CTS	MS	MS	CSIW

application has a relatively high gain due to the low ohmic losses of fixed-capacitor. The proposed antenna shows comparatively better performance and uses less number of varactor diodes compared with other EC applications. In addition, the proposed antenna is much easier to fabricate than other EC LWAs with continuous beam-steerable due to the single-layer structure and extremely simplified dc bias network.

IV. CONCLUSION

An EC LWA based on a CSIW with single-layer structure and extremely simplified dc bias network has been presented in this letter. Full-wave analysis of the proposed antenna shows that the radiation angle is from −58° to 48° when the capacitance from 0.3 pF to 0.55 pF at a fixed frequency. This antenna has been fabricated with varactor diodes loading and the fixed frequency beam scanning capability has been experimentally validated. By adjusting reverse bias voltage from 32 V to 7.5 V, the beam scans from −40.66° to 31.32° continuously, and the gains are almost better than 5 dB. The proposed LWA achieves a wide beam steering range about 72°. Finally, using varactor diodes with low ohmic losses can improve the antenna performance effectively.

REFERENCES

[1] A. A. Oliner and D. R. Jackson, *Antenna Engineering Hand Book*, 4th ed. New York, NY, USA: McGraw-Hill, 2007.
[2] D. R. Jackson, C. Caloz, and T. Itoh, "Leaky-wave antennas," *Proc. IEEE*, vol. 100, no. 7, pp. 2194–2206, Jul. 2012.
[3] F. Xu and K. Wu, "Understanding leaky-wave structures: a special form of guided-wave structure," *IEEE Microw. Mag.*, vol. 14, no. 5, pp. 87–96, Jul./Aug. 2013.
[4] D.-F. Guan, Q. Zhang, P. You, Z.-B. Yang, Y. Zhou, and S.-W. Yong, "Scanning rate enhancement of leaky wave antennas using slow-wave substrate integrated waveguide (SIW) structure," *IEEE Trans. Antennas Propag.*, vol. 66, no. 7, pp. 3747–3751, Jul. 2018.
[5] Y. Dong and T. Itoh, "Composite right/left-handed substrate integrated waveguide and half mode substrate integrated waveguide leaky-wave structures," *IEEE Trans. Antennas Propag.*, vol. 59, no. 3, pp. 767–775, Mar. 2011.

[6] D.-F. Guan, P. You, Q. Zhang, K. Xiao, and S. W. Yong, "Hybrid spoof surface plasmon polariton and substrate integrated waveguide transmission line and its application in filter," *IEEE Trans. Microw. Theory Techn.*, vol. 65, no. 12, pp. 4925–4932, Dec. 2017.

[7] D.-F. Guan, P. You, Q. Zhang, Z.-B. Yang, H. Liu, and S.-W. Yong, "Slow-wave half-mode substrate integrated waveguide using spoof surface plasmon polariton structure," *IEEE Trans. Microw. Theory Techn.*, vol. 66, no. 6, pp. 2946–2952, Jun. 2018.

[8] K. Chen, Y. Zhang, S. He, H. Chen, and G. Zhu, "A novel frequency scanning leaky-wave antenna based on corrugated substrate integrated waveguide," *Int. J. Antennas Propag.*, vol. 2018, 2018, Art. no. 5034721.

[9] L. Chang, Y. Li, Z. Zhang, and Z. Feng, "Reconfigurable 2-Bit fixed-frequency beam steering array based on microstrip line," *IEEE Trans. Antennas Propag.*, vol. 66, no. 2, pp. 683–691, Feb. 2018.

[10] Y. Li, M. F. Iskander, Z. Zhang, and Z. Feng, "A new low cost leaky wave coplanar waveguide continuous transverse stub antenna array using metamaterial-based phase shifters for beam steering," *IEEE Trans. Antennas Propag.*, vol. 61, no. 7, pp. 3511–3518, Jul. 2013.

[11] R. Guzman-Quiros, J. L. Gomez-Tornero, A. R. Weily, and Y. J. Guo, "Electronic full-space scanning with 1-D Fabry–Pérot LWA using electromagnetic band-gap," *IEEE Antennas Wireless Propag. Lett.*, vol. 11, pp. 1426–1429, 2012.

[12] S. Lim, C. Caloz, and T. Itoh, "Metamaterial-based electronically controlled transmission-line structure as a novel leaky-wave antenna with tunable radiation angle and beamwidth," *IEEE Trans. Microw. Theory Techn.*, vol. 52, no. 12, pp. 2678–2690, Dec. 2004.

[13] J. H. Fu, A. Li, W. Chen, B. Lv, Z. Wang, P. Li, and Q. Wu, "An electrically controlled CRLH-inspired circularly polarized leaky-wave antenna," *IEEE Antennas Wireless Propag. Lett.*, vol. 16, pp. 760–763, 2017.

[14] A. Suntives and S. V. Hum, "A fixed-frequency beam-steerable half-mode substrate integrated waveguide leaky-wave antenna," *IEEE Trans. Antennas Propag.*, vol. 60, no. 5, pp. 2540–2544, May 2012.

[15] A. Suntives and S. V. Hum, "An electronically tunable half-mode substrate integrated waveguide leaky-wave antenna," in *Proc. 5th Eur. Conf. Antennas Propag.*, Apr. 2011, pp. 3670–3674.

[16] K. W. Eccleston, "Mode analysis of the corrugated substrate integrated waveguide," *IEEE Trans. Microw. Theory Techn.*, vol. 60, no. 10, pp. 3004–3012, Oct. 2012.

[17] Z. Liu, G. Xiao and L. Zhu, "Numerical de-embedding and experimental validation of propagation properties of corrugated substrate integrated waveguide," *Microw. Opt. Technol. Lett.*, vol. 58, pp. 2456–2460, 2016.

[18] D. Deslandes and K. Wu, "Analysis and design of current probe transition from grounded coplanar to substrate integrated rectangular waveguides," *IEEE Trans. Microw. Theory Techn.*, vol. 53, no. 8, pp. 2487–2494, Aug. 2005.